Biomed Microdevices (2015) 17: 34
DOI 10.1007/s10544-015-9927-z

Coating flexible probes with an ultra fast degrading polymer to aid in tissue insertion

Meng-chen Lo · Shuwu Wang · Sagar Singh · Vinod B. Damodaran · Hilton M. Kaplan · Joachim Kohn · David I. Shreiber · Jeffrey D. Zahn

Published online: 15 February 2015

Abstract We report a fabrication process for coating neural probes with an ultrafast degrading polymer to create consistent and reproducible devices for neural tissue insertion. The rigid polymer coating acts as a probe insertion aid, but resorbs within hours post-implantation. Despite the feasibility for short term neural recordings from currently available neural prosthetic devices, most of these devices suffer from long term gliosis, which isolates the probes from adjacent neurons, increasing the recording impedance and stimulation threshold. The size and stiffness of implanted probes have been identified as critical factors that lead to this long term gliosis. Smaller, more flexible probes that match the mechanical properties of brain tissue could allow better long term integration by limiting the mechanical disruption of the surrounding tissue during and after probe insertion, while being flexible enough to deform with the tissue during brain movement. However, these small flexible probes inherently lack the mechanical strength to penetrate the brain on their own. In this work, we have developed a micromolding method for coating a non-functional miniaturized SU-8 probe with an ultrafast degrading tyrosine-derived polycarbonate (E5005(2K)). Coated, non-functionalized probes of varying dimensions were reproducibly fabricated with high yields. The polymer erosion/degradation profiles of the probes were characterized *in vitro*. The probes were also mechanically characterized in *ex vivo* brain tissue models by measuring buckling and insertion forces during probe insertion. The results demonstrate the ability to produce polymer coated probes of consistent quality for future *in vivo* use, for example to study the effects of different design parameters that may affect tissue response during long term chronic intra-cortical microelectrode neural recordings.

Keywords Microfabrication · Neural probe · Flexible probe · Biodegradable polymer

M.-c. Lo (✉) · S. Singh · D. I. Shreiber · J. D. Zahn
Department of Biomedical Engineering, Rutgers, the State University of New Jersey, Piscataway, NJ, USA
e-mail: vetdied@gmail.com

S. Wang · V. B. Damodaran · H. M. Kaplan · J. Kohn
New Jersey Center for Biomaterials, Rutgers, the State University of New Jersey, Piscataway, NJ, USA

1 Introduction

Brain computer interfaces (BCI) establish communication between the brain and external devices without transmission through peripheral neural pathways (Daly and Wolpaw 2008; Hochberg et al. 2006, 2012). There is rising interest and need for BCIs to assist people who have suffered from nervous system impairments (e.g., spinal cord injury, demyelination diseases, neurodegenerative diseases). The first step in this process is signal recording. It is, therefore, essential to develop suitable recording modalities that are capable of obtaining high quality, consistent signals, while facilitating long-term probe implantation to enable lifetime use of BCI devices. There has been extensive research on neural probe development, covering many different design aspects such as probe materials, probe dimensions, microfabrication processes, electrode dimensions and the electrode-cell interface (Lu et al. 2010; Ming et al. 2002; Pfurtscheller et al. 2000; Rousche and Normann 1998; Sun et al. 2014; Vaughan et al. 2003).

Pioneering neural recording studies used miniaturized 30 to 50 μm diameter metal wires made from platinum, iridium, copper or stainless steel and coupled with a Teflon or polyimide coating as insulation (Salcman and Bak 1973; Schmidt et al. 1976). Development of microfabrication techniques enhanced the capabilities of neural recording devices. Silicon microfabrication processes provide fine control over the probe

and electrode size, shape, spacing and even allow multiple recording sites to be fabricated within each probe to increase the device efficacy (Wise et al. 1970). Despite the feasibility for short term neural recordings (~2–6 weeks) (Rousche and Normann 1998; Williams et al. 1999) from these different types of probes, most of the devices ultimately failed due to disruption of the electrode-cell interface by the foreign body response, which alters the recording feasibility over time until the probes are finally no longer able to acquire stable and consistent signals (Edell et al. 1992; Kozai et al. 2012b; Lund et al. 2010; Polikov et al. 2005; Turner et al. 1999; Vetter et al. 2004; Wang and Thampatty 2008).

Two forms of tissue response cause this mode of failure: (1) *acute* activation of microglia and astrocytes (Polikov et al. 2005; Turner et al. 1999); (2) *chronic* glial scar formation (Biran et al. 2005; Szarowski et al. 2003). When neural probes are inserted into brain tissue, the mechanical trauma causes cellular damage and disruption of blood vessels which leads to astrocyte and microglia activation (Bjornsson et al. 2006; Fujita et al. 1998; Giordana et al. 1994), which interfere with microcirculation. Disruption of blood vessels releases erythrocytes, clotting factors, and inflammatory factors that facilitate macrophage recruitment and alter the probe's recording performance (Saxena et al. 2013; Turner et al. 1999). This acute inflammatory response usually subsides within 1 week post probe insertion (Fujita et al. 1998; Leskovar et al. 2000).

However, a chronic foreign body response can then be observed, presumably aggravated by continual shear forces of the brain moving relative to the rigid probes (Seymour and Kipke 2007; Szarowski et al. 2003). Most functional probe failures result from this long term CNS response, in which gliosis forms an encapsulation layer that isolates the electrodes from the adjacent neural cells (Edell et al. 1992; Rousche and Normann 1998; Szarowski et al. 2003; Turner et al. 1999). This encapsulation electrically insulates the probes, which impairs the devices by dramatically increasing their recording impedance (Mercanzini et al. 2009; Williams et al. 2007), and so decreasing the signal to noise ratio (SNR) (Edell et al. 1992; Vetter et al. 2004).

Larger devices (>100 μm wide long-term) are expected to cause more tissue disruption, chronic shear injury, and a foreign body response, and ultimately induce a more severe chronic glial encapsulation (Kipke et al. 2008; Kozai et al. 2012a; Seymour and Kipke 2007). It is hypothesized that creating miniaturized probes will help reduce the extent of both acute and chronic tissue response through minimizing insertion trauma (Ebersole 1997; Subbaroyan and Kipke 2006; Takeuchi et al. 2003). In the late 1990's, several groups suggested the fabrication of flexible probes from polymer materials to minimize tissue responses by aiming to mechanically match device compliance with that of adjacent tissues (Hoogerwerf and Wise 1994; Stieglitz et al. 1997; Takeuchi and Shimoyama 2000). Since then, more flexible materials have been used, including SU-8, polyimide or poly(p-xylylene) (parylene) to replace or improve recording ability compared to rigid silicon-based probes (Altuna et al. 2012; Cho et al. 2008; González and Rodríguez 1997; Smith et al. 2012). However, effective insertion of these flexible probes usually requires probes larger than their silicon counterparts and/or large insertion shuttles to aid in implantation.

Various insertion aids have been investigated to allow insertion of flexible probes. An ideal insertion aid will provide sufficient mechanical strength to penetrate the tissue in a narrow and sharp form factor to minimize the tissue response induced by insertion. Insertion aids made from stiffer materials such as needles or silicon shanks have been incorporated with the flexible probes as temporary insertion shuttles and are removed after implantation (Felix et al. 2013; Kim et al. 2013). However, those types of removable shuttles are usually stiffer and larger in size, and may therefore compromise short-term probe performance due to mechanical trauma.

One other method to stiffen flexible microprobes is to encapsulate the device within biodegradable polymers for insertion. Poly(ethylene glycol) (PEG) has been investigated as an insertion aid due to its biocompatibility and solubility in the tissue body fluids (Chen et al. 2009, 2011; Takeuchi et al. 2005); however PEG has limited rigidity and therefore requires thicker coatings or a shuttle to ensure successful insertion. Poly(D,L-lactide-co-glycolide) (PLGA) has also been used as an insertion aid for flexible parylene neural probes because it is both biocompatible and biodegradable and is widely used in biomedical applications (Foley et al. 2009). However, the degradation time of PLGA is around 3 to 4 weeks, which exceeds the time over which the acute and even chronic tissue responses occur. Carboxyl-methylcellulose (CMC) has also been proposed as a shuttle which can couple with neural probes for insertion (Gilgunn et al. 2012). It is bio-dissolvable and has also been proposed as a matrix for slow release of other molecules such as neural regenerative drugs to prevent tissue responses. However, when tested, the CMC composite was reported to become gel-like instead of completely degrading within the body, thereby potentially limiting the proximity of neural units.

More recently, there are groups fabricating probes using novel materials where the stiffness is reduced following device implantation. One example is the fabrication of devices out of shape memory polymers that are stiff during implantation and soften *in vivo* to approach the brain tissue modulus (Ware et al. 2012). However, the device stiffness (shear modulus ~700 MPa) prior to insertion is still less than silicon (~200 GPa) and therefore a larger device is required to ensure successful implantation. A mechanically adaptive polymer nanocomposite probe has been fabricated via film casting (Harris et al. 2011; Nguyen et al. 2014). The material is capable of decreasing its tensile modulus from 5 GPa pre-insertion to 12 MPa post-insertion within 15 minutes under

physiological conditions. However, since the study examined the implants without electrode traces, future investigation may be needed to ensure that the nanocomposite casting procedure can accommodate the patterning of recording elements.

In this work, we have developed a micromolding method for coating a non-functional miniaturized SU-8 probe with an ultrafast degrading tyrosine-derived polycarbonate (E5005(2K)). The polymer is both biocompatible and biodegradable, and degrades into non-toxic, resorbable tyrosine and PEG by-products that have no harmful effects (Bourke and Kohn 2003; Hooper et al. 1998). Furthermore, the degradation rate of the polymer is easily tunable by variations in the polymer composition (Ertel and Kohn 1994; Hooper et al. 1998). This polymer is stiffer than PEG on its own, and provides sufficient strength for device implantation followed by an ultra-fast (~1–2 h) degradation and resorption that leaves only the microprobe inserted within the tissue (Lewitus et al. 2011). Previous work by our group (Lewitus et al. 2011) used a dip coating to coat the probe. The coating dimensions were less defined and usually thicker than what is required for insertion. For this study, we designed a proof-of-concept fabrication process adapting the water and temperature sensitive characteristics of the polymer to produce devices with more defined probe and coating dimensions. Specifically, SU-8 probes with different probe and coating dimensions were fabricated. The polymer coated probes were chemically characterized to investigate the coating polymer resorption profile and verify that the probe remained intact after the polymer degraded. The probes were also mechanically examined for buckling force to evaluate the probe integrity. We expect this coating procedure can be further utilized to coat probes of varying dimensions fabricated from a variety of different materials such as SU-8, parylene or polyimide.

2 Materials and methods

2.1 Polymer preparation

The tyrosine-derived polycarbonate based co-polymer used for coating was synthesized at the New Jersey Center for Biomaterials according to previously published procedures (Rojas et al. 2009; Schut et al. 2007) from 3 monomers: desaminotyrosyl-tyrosine alkyl ethyl ester (DTE), desaminotyrosyl-tyrosine (DT), and low-molecular-weight poly(ethylene glycol) (PEG). The naming convention for this type of polymer is EXXYY(MW), meaning poly(DTE-co-XX%DT-co-YY%-PEGMW carbonate) where XX is the mole percent of DT, YY is the mole percent of the PEG and the MW is the average molecular weight of the PEG (Fig. 1). The mechanical and chemical properties of these polymers depend on the polymer composition and relative molar percentages of the three monomers. The DTE component provides strength and stability, the DT component determines resorption rate and has a carboxyl group that allows functionality, and the PEG component determines resorbtion rate. The polymer degrades via hydrolysis of the carbonate linkages. The incorporation of DT and PEG in the polymer backbone makes the polymer more hydrophilic, enhancing the degradation rate by allowing faster water absorption. The specific type of polymer that was primarily used is E5005(2K) (E= 1.6 GPa, T_g=57 °C, M_n=100 K) which is 50 % DT, 5 % PEG. The E5005(2K) composition was found to have the proper mechanical and chemical qualities desired for an insertion aid, in that it has a fairly high Young's modulus (E=1.6 GPa), while being able to chemically degrade fully within a few hours (Lewitus et al. 2011).

2.2 SU-8 non-functional probe fabrication and polymer coating procedure

2.2.1 Polymer coated SU-8 probe fabrication

SU-8 was chosen as a test material on which to develop the coating procedure. The microprobe fabrication can be split into two parts: 1) Polymer coating mold fabrication; 2) Probe fabrication and polymer coating. The polymer coating mold was fabricated via a standard photolithography process. A thick negative photoresist (SU-8 2075) was spin-coated (1000 rpm) on a silicon substrate to the desired thickness (100 μm). The molding structure was defined and patterned by photolithography. Polydimethylsiloxane (PDMS) was poured over the master to create the molding cavity through soft lithography. After curing, the PDMS molding structure was removed from the wafer and a hole was drilled through the anchoring area as a solution inlet for use in the downstream polymer coating process.

PDMS was chosen as a substrate layer for probe fabrication to take advantage of the weak adhesion between PDMS and SU-8. This allowed for the SU-8 device to be lifted from the substrate while still providing support to carry out photolithography to define the probe structure. To prevent significant contraction of SU-8 layer during baking because of rapid solvent evaporation, a special soft baking recipe at a lower temperature for a longer baking time was conducted. This ensured the desired uniform coating of SU-8 on top of the PDMS substrate (Fig. 2). First, PDMS was mixed with the curing agent at 10:1 weight ratio for substrate coating. A thin layer of PDMS (65 μm) was spin-coated (2000 rpm) on top of the glass substrate, and baked for 5 min to cure the PDMS. Second, a thin layer of SU-8 (SU-8 2010; 10–20 μm thick) was spin-coated on top of the cured PDMS substrate layer. The whole device was then baked at 30, 35, 40, 45, 50, 55, 60 and 65 °C for 5 minutes at each temperature, and then cooled to room temperature for at least 1 hour before downstream exposure. The SU-8 was then patterned to the probe

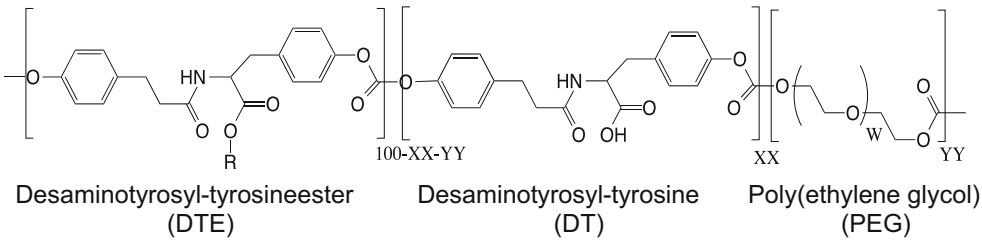

Fig. 1 Chemical structure of the tyrosine-derived polycarbonate (Poly (DTE-co-XX%DT-co-YY%PEG(Wk)))

geometries with standard photolithography. The probe was imaged using scanning electron microscope (SEM) (AMRAY-1830I, AMRAY, Bedford, MA, USA) to ensure probe integrity prior to polymer coating. Following probe definition, the PDMS molding piece, previously fabricated, was aligned with the SU-8 probe under a light microscope, and pressed onto the substrate to form a conformal contact and a molding capillary.

The E5005(2K) polymer solution was infused from the molding inlet to coat the probe using the micromolding in capillaries (MIMIC) (Kim et al. 1996) process, where polymer solution is introduced into a microchannel reservoir and fills the cavities through capillary action. The E5005(2K) polymer solution was prepared as 9 % *w/w* in anhydrous 1, 4-dioxane (Sigma-Aldrich, St. Louis, MO, USA). To start the coating process, 5 μL of polymer solution was introduced through the reservoir inlet twice at room temperature. The whole device was then placed on a 75 °C hotplate, and 5 μL of the polymer solution was introduced 3 times at 5 minutes intervals. The device remained on the hotplate for another 2 hours to drive off the solvent. To slowly and completely evaporate the solvent within the polymer, the whole device was placed under −15 mmHg vacuum at 50 °C for an hour, and finally in full vacuum (−30 mmHg) for at least 1 day. The vacuum was increased slowly to remove any air bubbles and prevent cavitation of the solvent and improve the coating quality. Finally, the PDMS molding structure was peeled off from the PDMS substrate and physically lifted away using tweezers. The coated probes were then stored in 24-well cell plates that were vacuum sealed and stored in a −20 °C freezer until downstream characterization to prevent polymer degradation from ambient humidity. For testing, probes were returned to room temperature under vacuum for 15 minutes and fixed on a glass slide.

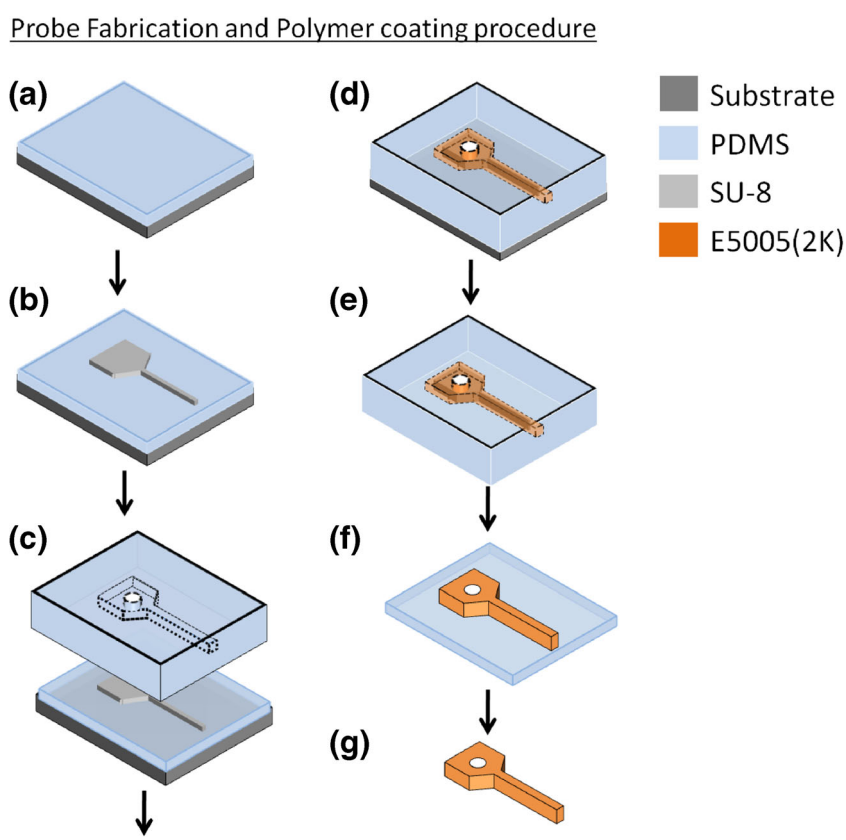

Fig. 2 Schematic of polymer coating fabrication process. **a** thin layer of PDMS (~65 μm) is spin coated on to a substrate. **b** The probe geometry is patterned on top of the PDMS layer. **c** The SU-8 probe is aligned with the molding structure. **d** Polymer solution is infused through the inlet of the mold using MIMIC technique and the polymer solvent is allowed to evaporate.
e The device is released from the substrate. **f** The device is released from the molding structure. **g** The device is lifted mechanically off from the PDMS substrate

2.3 Chemical characterization of the coated probe

2.3.1 Polymer erosion profile in PBS

Two coated probe candidates (coating dimensions: 100 or 150 μm wide, 3.5 mm long, 100 μm thick; probe dimensions: 30 μm wide, 3 mm long, 10 μm thick) were evaluated to assess how quickly the polymer (E5005(2K)) erodes over time using a spectrophotometer (Varian Cary 50 Bio UV/Visible Spectrophotometer, Varian Inc, Palo Alto, CA, USA) to measure UV absorbance of the samples. A 3.5 mL cuvette was filled with 3 mL of 10 mM Phosphate Buffered Saline (PBS; pH 7.4, Life Technologies, Grand Island, NY, USA),which was analyzed as a control before adding the probe to the cuvette. The sample was kept at 37 °C in a water bath during the study except during data acquisition. Samples were retrieved from the bath and analyzed every 10 minutes until the UV absorbance reached a steady state absorbance. E5005(2K) is a tyrosine derived polycarbonate and therefore UV absorbance of the polymer is comparable to tyrosine, which is around 260 nm (Goodwin and Morton 1946). UV absorbance in the 240 to 300 nm wavelength range was measured and monitored at each time point. The absorbance data was then processed and normalized against the maximum absorbance during the whole recording session.

2.3.2 In vitro polymer erosion profile in agarose phantom

The polymer erosion/degradation profile was further examined using an *in vitro* brain tissue phantom to simulate physiological conditions. To visualize the polymer degradation/erosion process, the polymer was first covalently labeled with a fluorescent dye, 1-pyrenyldiazomethane (PDAM), by dissolving 168 mg of E5005(2K) polymer in 5 mL tetrahydrofuran (THF), adding 0.69 mg of PDAM in dichloromethane, and incubating overnight. The solvent was then evaporated at room temperature, and the polymer was further dried under vacuum for 3 days at room temperature. The fluorescently labeled polymer solution (9 % *w/w* in anhydrous 1,4-dioxane) was used to coat the probe using the procedure previously described, and the coated probes were covered with aluminum foil to prevent fluorescent dye from photobleaching until testing. The coated probes were inserted into a 1 % agarose gel phantom (Chen et al. 2004) slowly by hand and kept in a 37 °C humidified incubator. Fluorescent images were obtained and monitored using an inverted microscope (Axio Observer-D1, Carl Zeiss MicroImaging GmbH, Göttingen, Germany) with a 10× objective in epifluorescent mode at different time points. The camera exposure was kept constant throughout the study. A similar procedure was used for labeling and monitoring a non degradable control polymer E1001(1K) (E=1.8 GPa, T_g=96 °C, M_n=160 K) with PDAM. The degradation profiles of E5005(2K) and E1001(1K) coated probes were quantified by performing intensity profile analysis over time using ImageJ. The intensity was normalized to the maximum intensity value within the same experiment for comparison.

2.4 Mechanical characterization of the coated probe

2.4.1 Theoretical rigidity estimation of the coated probes

Fabricated polymer coated probes were characterized mechanically by measuring the buckling force and comparing the force limits with theoretical estimates. Axial insertion of a probe is expected to cause failure via buckling. The buckling force that a given probe can withstand can be calculated with Euler's buckling Eq. (1), where E is the Young's modulus of the coating material, I is the area moment of inertia which is defined by the cross-sectional area (width and height) of the probe, L is the unsupported length of the column, and K is the column effective length factor, which is determined based upon the boundary condition at each end of the probe. When coated probes are inserted into an agarose gel, one end is fixed by the insertion apparatus and the other end is pinned once it makes contact with the gel, whereafter it cannot move laterally but is free to rotate. For this condition, K has a value of 0.6999 (Kishi et al. 1997). The moment of inertia depends on the geometry of the probe. The probe was assumed to be a rectangular beam, where h is the thickness of the probe and b is the width of the probe (2). By substituting (2) into (1), a buckling force equation related to probe geometry can be obtained (3). The Young's modulus of the polymer (E5005(2K):1.64 GPa) was found experimentally from uniaxial tension experiments. The coated probe was assumed to be a solid polymer beam without the actual encapsulated probe, which may slightly overestimate the actual probe strength given the relative stiffness of the two materials.

$$F = \frac{\pi^2 EI}{(KL)^2} \tag{1}$$

$$I = \frac{bh^3}{12} \tag{2}$$

$$\mathrm{F} = \frac{\pi^2 \mathrm{Ebh}^3}{5.88\mathrm{L}^2} \tag{3}$$

2.4.2 Ex vivo mechanical testing of the coated probes

The mechanical integrity of the polymer-coated probes was first characterized in *ex vivo* chick embryonic brains. Fresh fertilized eggs (Charles River Labs, MA, USA) were incubated until embryonic day 18 (full gestation is 22 days), after

which the brains were extracted and placed in 37 °C PBS solution. Buckling and insertion force measurements were performed with a Bose/Enduratec ELF 3200 uniaxial testing system (ELF 3200, Bose, MN, USA).

In the experimental setup, the probe was secured to a 0.5 N cantilever load cell (Entran Sensors and Electronics, NJ, USA). The brain was fixed so that the cortical surface faced upward and was not allowed to move during the insertion. A level was used to confirm the probe was perpendicular to the testing platform and positioned so that insertions occurred around the motor cortex region, where the brain is the most flat. The probe was lowered at a rate of 0.1 mm/s into the brain tissue. Four insertions were performed per brain in different locations. For cases where the probe withstood the penetration force, the buckling force was measured when the probe made contact with the bottom surface of the fixture holding the brain. In total, buckling forces were measured on twenty-two coated probes with different dimensions (100, 150, and 200 μm wide, 100 μm thick and 3.5 mm long). To prevent dehydration-induced alterations of material properties, brains were discarded every 15 min and replaced with freshly extracted samples. After the experiments, data were processed using Matlab, and experimental buckling force measurements were compared with the theoretical estimations.

In separate tests, the coated probes were inserted into a fresh *ex vivo* adult rat brain (Sprague–Dawley rat; Charles River Labs, MA, USA). The animal was euthanized by asphyxiation in 100 % CO_2 environment under an approved IACUC protocol. The rat brain was extracted with the pia mater remained, but the dura mater was removed with the overlying skull. Buckling and insertion forces were tested on eleven uncoated SU-8 probes (30 μm wide × 10 μm thick × 3.0 mm long) and twelve coated probes (polymer coating : 100 μm wide × 100 μm thick × 3.5 mm long) using the methods described above. A humidifier was used to maintain the brain's hydration during the experiment, which was carried out at ambient temperature. To minimize potential changes in the mechanical properties of the *ex vivo* brain tissue, all experiments were completed within 45 min post extraction.

3 Results and discussion

3.1 SU-8 non-functional probe fabrication and polymer coating procedure

Different non-functional SU-8 probes with widths varying from 20 to 40 μm and thicknesses of 10 or 20 μm were fabricated. Figure 3a displays a SEM image of the non-functional SU-8 probe on a PDMS substrate. The prolonged, gradient, and low temperature soft baking recipe, which prevents SU-8 shrinkage on the PDMS substrate, did not affect the final probe integrity. The large pentagon shaped area defined the handling area for integration with other instrumentation, such as a mechanical support for handling or electrical integration for signal recording. The cross marks aided in aligning the molding structure for polymer coating. A weak point that caused fabrication failure was noted at the transition between the anchoring area and the probe shank, where most of the mechanical disruption occurred as the structure was peeled from the substrate. SU-8 probe integrity was therefore maintained by a smooth transition between the anchoring area and the probe shank. SU-8 exhibits a high residual stress following exposure that may result in a rough surface on the probe itself or distortion of the probe shaft once released from the substrate. Therefore, alternative and more biocompatible materials, such as parylene, will be used in the future to fabricate functional probes.

The ideal polymer coating should yield an uniform coating and smooth surface to minimize the amount of tissue disruption upon insertion that can lead to both acute and chronic tissue responses. Figure 3b shows a light microscopy image of a coated probe that has been lifted from the PDMS substrate and fixed on a glass slide. The SU-8 probe can be clearly identified in the middle of the polymer shank, without material disruption or damage during fabrication and device lift-off. Figure 3c displays a SEM micrograph of the coated probe from the back. The bottom side of the SU-8 probe was not coated with polymer due to attachment between the probe and the substrate. The SU-8 probe shape can be identified within the polymer shank, and the polymer coating was smooth and rigid, indicating that there was no material disruption between the coating and probe during encapsulation.

One design consideration for this work is the need to ultimately remove the coated probe from the supporting substrate following fabrication. Most polymer neural probes are usually removed from their substrate through dissolution of a sacrificial layer patterned under the device. However, due to the chemical characteristics of the tyrosine-derived polycarbonate, most organic and aqueous solutions will cause the E5005(2K) polymer to degrade/erode. Therefore, releasing the final device through wet chemical etching of a sacrificial layer has proved impractical, compared to mechanical lift-off methods. PDMS was used as the supporting layer, allowing the whole device to be mechanically peeled from the substrate (Patel et al. 2008). However, mechanical peeling methods are not optimal as they could physically damage the coated probe. As an alternative, xenon difluoride etching of the substrate was also identified as a dry etchant to release the probe (Chang et al. 1995; Zhu et al. 2007). XeF_2 is a dry, isotropic, vapor-phase etch that is highly selective to silicon with respect to aluminum, photoresist and silicon dioxide, and the etch rate is about 2 μm/min. It is a white crystalline solid at room

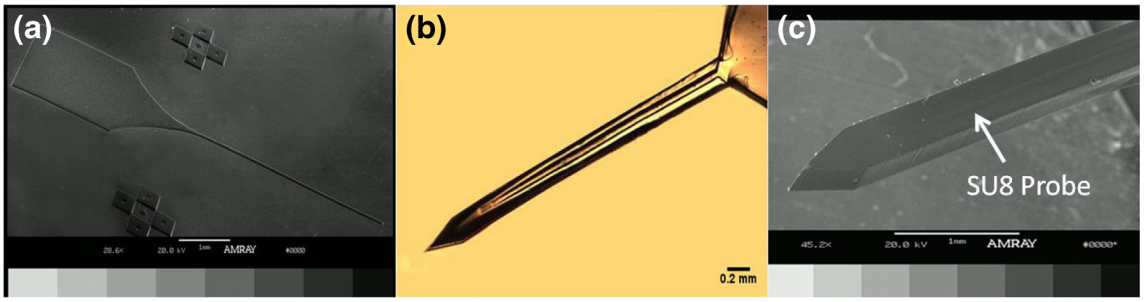

Fig. 3 **a** SEM micrograph of a non-functional SU-8 probe. Probe dimension: 30 μm wide, 20 μm thick and 3 mm long. **b** Light microscope image of the coated probe. **c** SEM micrograph of the coated probe. Device dimension: polymer shank: 200 μm wide, 100 μm thick and 3.5 mm long. SU-8 probe: 30 μm wide, 20 μm thick and 3 mm long

temperature and atmospheric pressure, but sublimates at its vapor pressure of 3.8 mmHg at 25 °C. It is being investigated as a future release candidate due to its high selectivity and its vapor-phase isotropic etching characteristics which allow undercutting of large structures.

3.2 Chemical characterization of the coated probe

3.2.1 Polymer erosion profile in PBS

Figure 4 displays relative mass retention in percentage over time with the two different coated probe candidates (with 100 or 150 μm wide coatings). The relative mass retention percentage was calculated according to the UV absorbance that increases as the polymer dissolves within the PBS. Approximately 50 % polymer dissolution occurred in PBS within 20 minutes. Steady state absorbance, indicating complete erosion/degradation of the polymer, was reached at nearly 60 minutes for both of the coated probes. There was no significant difference between the two samples on the rate of polymer degradation/erosion with coating size, at such a small scale. Moreover, the rate of degradation/erosion is proportional to the contact area between the probe and aqueous solution, which means the larger the polymer coating, the faster the degradation/erosion rate. This effect may offset the larger mass that would otherwise take more time to degrade.

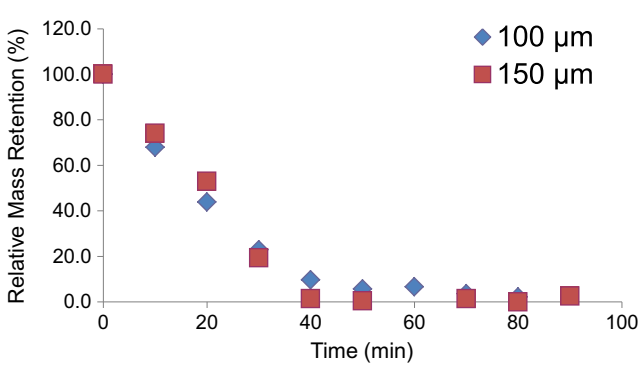

Fig. 4 Relative mass retention of the E5005(2K) coated probe with different probe candidates. Device dimension: polymer shank: 100 or 150 μm wide, 100 μm thick and 3.5 mm long. SU8-probe: 30 μm wide, 20 μm thick and 3 mm long

3.2.2 Polymer erosion profile in brain tissue phantom

Polymer degradation/erosion profiles were compared between probes coated with E5005(2K) (ultrafast degrading) and E1001(1K) (slow-degrading). Figure 5 shows time lapse images of the SU-8 probes coated with each polymer, as well as quantitative intensity profiles indicating polymer degradation/erosion at different time points. Degradation and erosion can be seen in the intensity change over time. Meanwhile, diffusion of the polymer into the gel can be observed from the expansion of the fluorescent region surrounding the probe.

Rapid erosion/degrade was observed with the probe coated with E5005(2K) (Fig. 5a). As shown in Fig. 5c, the E5005(2K) started to erode (intensity dropping from 100 to ~ 60 %) as soon as the probe was inserted into the 1 % agarose gel. Fifteen minutes after insertion, the polymer has eroded and diffused away from the center of the SU-8 probe with the peak intensity remained roughly the same. Sixty minutes after insertion, the intensity has dropped to ~10 % and more diffused away (~200 μm) from the center of the SU-8 probe. The polymer has completely eroded from the probe and diffused into the agarose gel with minimal fluorescence signal observed after 120 minutes. The SU-8 probe can be clearly identified in the image after 120 minutes without mechanical or material disruption indicating the polymer coating and erosion/degradation did not affect probe integrity.

In contrast, the intensity for E1001(1K) between 0 and 30 minutes was approximately the same, indicating minimal erosion 30 minutes after insertion (Fig. 5b and d). The polymer remained 20 hours after insertion and was found to swell and expand, but did not diffuse away from the probe. Interestingly, the intensity was found to be higher 20 hours after device insertion. This may be due to differences in the degradation and erosion rates, which may have led to an observable overlap of fluorescence in different layers of the slow-degrading polymer. Regardless, the experiment

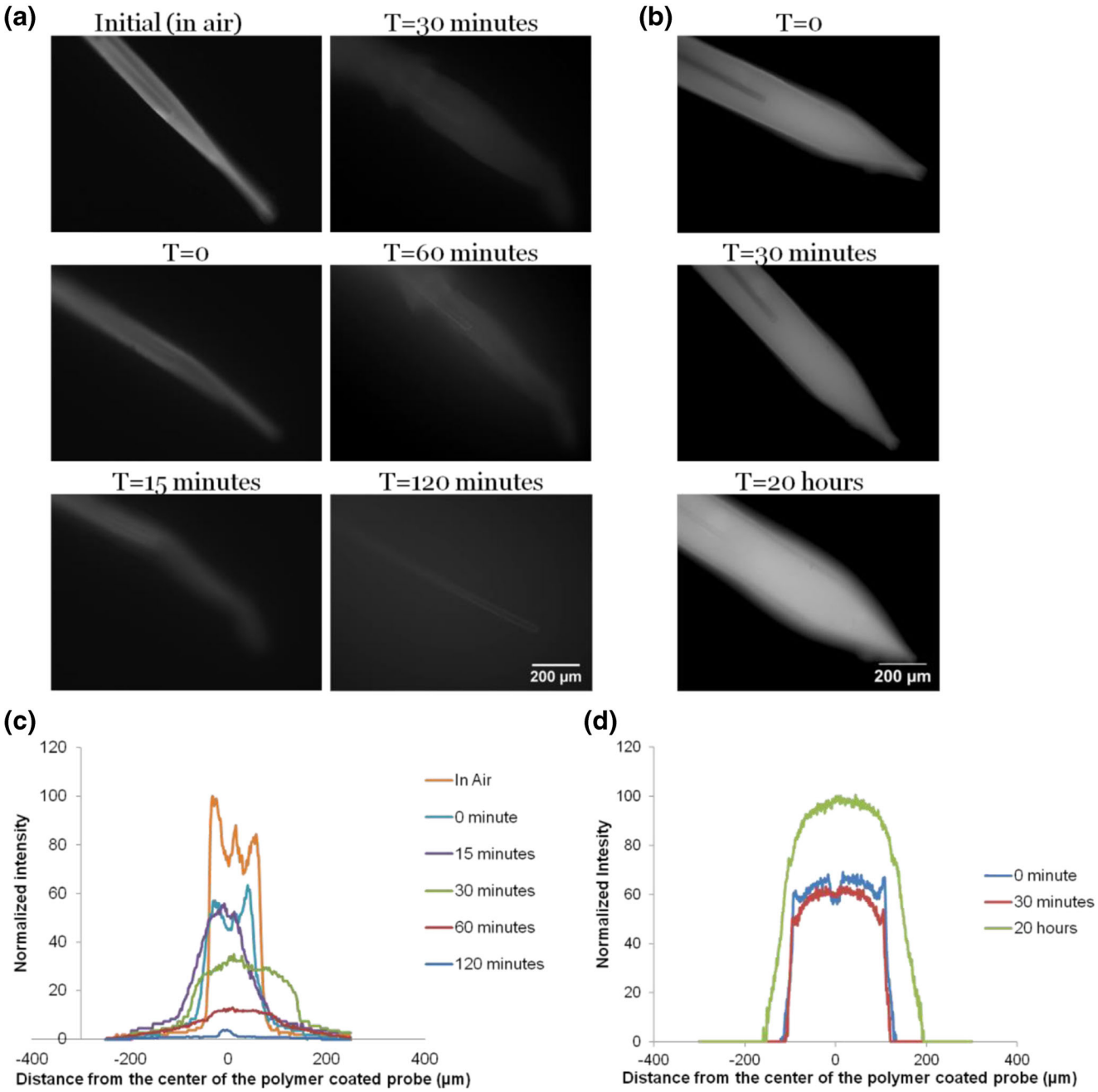

Fig. 5 Time lapse fluorescent images of SU-8 probe coated with (a) E5005(2K) and (b) E1001(1K). Device dimension: **a** polymer shank: 100 µm wide, 100 µm thick and 3.5 mm long. SU8-probe: 30 µm wide, 20 µm thick and 3 mm long. **b** Polymer shank: 200 µm wide, 100 µm thick and 3.5 mm long. SU-8 probe: 30 µm wide, 20 µm thick and 3 mm long. **c** Intensity profile for E5005(2K) coated probe over different time points from the center of the probe.**d** Intensity profile for E1001(1K) coated probe over different time points from the center of the probe

confirmed that the E5005(2K) coated SU-8 probe was able to penetrate the phantom brain tissue surrogate without device disruption and polymer degraded/erode within 2 hours leaving the probe intact within the tissue.

The main mechanism for the polymer degradation is hydrolysis with the addition of water. A 1 % agarose gel was used as the brain phantom for this study, which contains less water compared to commonly used brain phantom agarose (0.6 % gel) (Chen et al. 2004). Therefore, the polymer degradation time is considered to be slower than *in vivo* environment. Chemical characterizations of the polymer coated probe within both PBS and 1 % agarose gel identify an estimated time window (60–120 minutes) for complete polymer degradation. Therefore, the experimental results can serve as a reference to inform a future *in vivo* polymer degradation study on when to sacrifice the animal for investigation.

3.3 Mechanical characterization of the coated probe

Mechanical testing was performed to evaluate the performance of the polymer coated probes. SU-8 was chosen as the probe material due to the ease of integration with the molding process. The Elastic Modulus of SU-8 (2 GPa) is comparable with commonly used polymer substrates such as parylene (2.8 GPa) and polyimide (2.5 GPa). Therefore SU-8 is an adequate surrogate material for this study. Although neural probes with sufficient stiffness for tissue insertion can be fabricated from each of these materials, these probes are much larger than is desired for minimizing shear injury and foreign body response post implantation. Therefore, we produced SU-8 probes which were 30 μm wide, 10 or 20 μm thick and 3 mm long where we expected a high degree of failure in the absence of a coating. These SU-8 probes were incorporated with E5005(2K) without any delamination between the two materials. Future work will be needed to confirm the adhesion between the polymer and more biocompatible materials such as parylene. Figure 6 shows the experimental and theoretical buckling force measurements for varying polymer coating widths. The error bar corresponds to the standard error (n= 22). The experimental buckling forces for 100, 150, and 200 μm coating widths (100 μm thick and 3.5 mm long) were slightly larger than the theoretical values, while the experimental buckling forces for 250 μm coating width was less than the theoretical value. The differences between the theoretical and calculated buckling forces may be attributed to slight variations in the coating dimensions. Additionally, each probe was exposed to the ambient environment for 1–3 minutes as it was fixed for mechanical insertion. Since the E5005(2K) polymer is very sensitive to humidity, the polymer may have swelled slightly during this time, thus potentially altering the material and mechanical properties. Further investigation may be needed to characterize possible mechanical property changes over time under different ambient conditions, and to determine the maximum duration that the probes can remain unpackaged before implantation. Such information would be essential when designing experimental protocols for future *in vivo* studies.

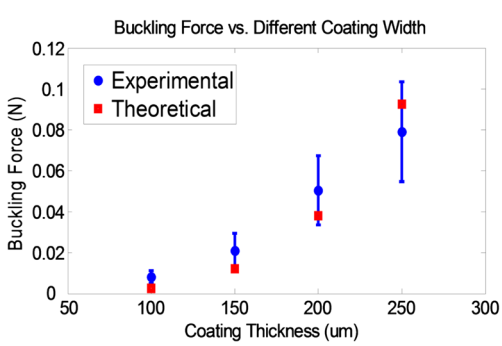

Fig. 6 Experimental and theoretical buckling force measurements vs. different coating widths. Device dimension: polymer Shank: 100, 150 , 200 and 250 μm wide, 100 μm thick and 3.5 mm long. SU-8 probe: 30 μm wide, 20 μm thick and 3 mm long

Buckling forces measured for smaller polymer coatings (100, 150 μm widths) were more accurate compared to the larger polymer coatings (200, 250 μm widths). The coating quality of smaller dimension devices was smoother and exhibited fewer defects due to a more constrained cavity during the coating procedure that made the polymer solution dry and solidify into a more uniform structure. However, despite the variances of coating qualities, the buckling force measurements fell within the standard deviation of the theoretical estimates with reasonable accuracy (<10 %).

To further validate the functional performance of the coated probes, the probes were also inserted into the fresh rat brain. Table 1 displays the successful insertion rate for uncoated SU-8 probes and E5005(2K) coated SU-8 probes. Approximately 55 % of the uncoated SU-8 probes were able to penetrate the brain tissue without buckling, implying that a more miniaturized device may be developed with the aid of polymer coating. Conversely, 100 % insertion success was achieved using E5005(2K) coated probes. It is noted that the Young's Modulus of SU-8 (2 GPa) and E5005(2K) (1.6 GPa) are very similar, indicating that the mechanism for stiffening is the ability to temporarily provide a thick insertion shuttle rather than to increase the effective modulus of the probe. Further experiments can be performed to determine the minimum coating dimensions that are still capable of providing 100 % insertion success.

Finally, insertion forces of identically sized probes (100 μm wide × 100 μm thick and 3.5 mm) were compared between the chicken embryonic and rat models. The average insertion force in the chicken embryonic model (4.55 mN) was similar to the force in the rat model (4.26 mN), indicating consistency among the coated probes and therefore confirming the repeatability of the fabrication procedure.

The current SU-8 probe candidates are 30 μm wide, 10 or 20 μm thick and 3 mm long. Most conventional neural probes have impedances around 1 MΩ at 1 kHz. Previous studies have shown that a recording area of 400 to 600 μm^2 is typical in order to obtain approximately 1 MΩ impedance (Abidian and Martin 2009; Takeuchi et al. 2003). To maintain recording feasibility while minimizing probe size, the width of the probe will likely be kept to at least 20 μm so that a 400 μm^2

Table 1 Insertion successful rate for uncoated SU-8 probe (30 μm wide, 10 μm thick and 3 mm long) and E5005(2K) coated SU-8 probe (Probe: 30 μm wide, 10 μm thick and 3 mm long 100 μm wide. Polymer coating: 100 μm wide, 100 μm thick and 3.5 mm long)

	Pass	Fail
SU-8 uncoated probe	6	5
E5005(2K) coated probe	12	0

recording electrode, whereas the probe thickness can be further miniaturized (~5 μm).

4 Conclusion and future work

Smaller and more flexible neural probes are hypothesized to allow better long term integration with neural tissue by limiting the mechanical disruption of tissue and long-term shearing by being flexible enough to deform with the surrounding brain tissue during movement. However, such devices require insertion aids to provide enough mechanical support to penetrate the brain. In this work, a fabrication procedure was reported that produces miniaturized probes with a tyrosine-derived polycarbonate coating which provides sufficient rigidity for device insertion while degrading quickly (within hours) to enable long-term neural signal recordings. PDMS was used as the substrate to provide sufficient bonding to conduct photolithography for probe fabrication and polymer coating, while still allowing mechanical lifting off of the device. The polymer coated probes were mechanically characterized *ex vivo* to confirm probe performance. They were also characterized chemically to confirm that the polymer coatings eroded within 2 hours while leaving the probe intact. This work also demonstrates the ability to reproduce consistent polymer-coated probes.

Future work includes adapting the fabrication process reported here to develop polymer-coated probes made from more inert and biocompatible materials such as parylene. Following characterization of the probes to identify suitable device dimensions, the microfabrication process will be expanded to functionalize the probes to create electrodes for signal recording. Finally, the functionalized, polymer-coated electrodes will be implanted *in vivo* to assess glial tissue response, which will allow further refinement of the device design and insertion protocol.

Acknowledgments This work is supported by New Jersey Commission on Spinal Cord Research Award #CSCR12IRG001.

References

M.R. Abidian, D.C. Martin, Adv. Funct. Mater. **19**, 573 (2009)
A. Altuna, L. Menendez de la Prida, E. Bellistri, G. Gabriel, A. Guimerá, J. Berganzo, R. Villa, L.J. Fernández, Biosens. Bioelectron. **37**, 1 (2012)
R. Biran, D.C. Martin, P.A. Tresco, Exp. Neurol. **195**, 115 (2005)
C.S. Bjornsson, S.J. Oh, Y.A. Al-Kofahi, Y.J. Lim, K.L. Smith, J.N. Turner, S. De, B. Roysam, W. Shain, S.J. Kim, J. Neural Eng. **3**, 196 (2006)
S.L. Bourke, J. Kohn, Adv. Drug Deliv. Rev. **55**, 447 (2003)
F.I. Chang, R. Yeh, G. Lin, P.B. Chu, E.G. Hoffman, E.J. Kruglick, K.S.J. Pister, M.H. Hecht, 117 (1995)
Z.-J. Chen, G.T. Gillies, W.C. Broaddus, S.S. Prabhu, H. Fillmore, R.M. Mitchell, F.D. Corwin, P.P. Fatouros, J. Neurosurg. **101**, 314 (2004)
C.-H. Chen, S.-C. Chuang, Y.-T. Lee, S.-R. Yeh, Y.-C. Chang, D.-J. Yao, in *Nano/Molecular Med. Eng. (NANOMED), 2009 I.E. Int. Conf.* (2009), pp. 278–281
C.-H. Chen, S.-C. Chuang, H.-C. Su, W.-L. Hsu, T.-R. Yew, Y.-C. Chang, S.-R. Yeh, D.-J. Yao, Lab Chip **11**, 1647 (2011)
S.-H. Cho, H.M. Lu, L. Cauller, M.I. Romero-Ortega, J.-B. Lee, G.A. Hughes, IEEE Sensors. J. **8**, 1830 (2008)
J.J. Daly, J.R. Wolpaw, Lancet Neurol. **7**, 1032 (2008)
J.S. Ebersole, J. Clin. Neurophysiol. **14**, 470 (1997)
D.J. Edell, V.V. Toi, V.M. McNeil, L.D. Clark, Biomed. Eng. IEEE Trans. **39**, 635 (1992)
S.I. Ertel, J. Kohn, J. Biomed. Mater. Res. **28**, 919 (1994)
S.H. Felix, K.G. Shah, V.M. Tolosa, H.J. Sheth, A.C. Tooker, T.L. Delima, S.P. Jadhav, L.M. Frank, S.S. Pannu, J. Vis. Exp. e50609 (2013)
C. Foley, N. Nishimura, K. Neeves, C. Schaffer, W. Olbricht, Biomed. Microdevices **11**, 915 (2009)
T. Fujita, T. Yoshimine, M. Maruno, T. Hayakawa, Acta Neurochir. (Wien) **140**, 275 (1998)
P.J. Gilgunn, R. Khilwani, T.D. Y. Kozai, D.J. Weber, X.T. Cui, G. Erdos, O.B. Ozdoganlar, G.K. Fedder, in *Micro Electro Mech. Syst. (MEMS), 2012 I.E. 25th Int. Conf.* (2012), pp. 56–59
M.T. Giordana, A. Attanasio, P. Cavalla, A. Migheli, M.C. Vigliani, D. Schiffer, Neuropathol. Appl. Neurobiol. **20**, 163 (1994)
C. González, M. Rodríguez, J. Neurosci. Methods **72**, 189 (1997)
T.W. Goodwin, R.A. Morton, Biochem. J. **40**, 628 (1946)
J.P. Harris, J.R. Capadona, R.H. Miller, B.C. Healy, K. Shanmuganathan, S.J. Rowan, C. Weder, D.J. Tyler, J. Neural Eng. **8**, 066011 (2011)
L.R. Hochberg, M.D. Serruya, G.M. Friehs, J.A. Mukand, M. Saleh, A.H. Caplan, A. Branner, D. Chen, R.D. Penn, J.P. Donoghue, Nature **442**, 164 (2006)
L.R. Hochberg, D. Bacher, B. Jarosiewicz, N.Y. Masse, J.D. Simeral, J. Vogel, S. Haddadin, J. Liu, S.S. Cash, P. van der Smagt, J.P. Donoghue, Nature **485**, 372 (2012)
A.C. Hoogerwerf, K.D. Wise, IEEE Trans. Biomed. Eng. **41**, 1136 (1994)
K.A. Hooper, N.D. Macon, J. Kohn, J. Biomed. Mater. Res. **41**, 443 (1998)
J. Subbaroyan D.R. Kipke, in *Eng. Med. Biol. Soc. 2006. EMBS'06. 28th Annu. Int. Conf. IEEE* (2006), pp. 3588–3591
E. Kim, Y. Xia, G.M. Whitesides, J. Am. Chem. Soc. **118**, 5722 (1996)
B.J. Kim, J.T.W. Kuo, S.A. Hara, C.D. Lee, L. Yu, C.A. Gutierrez, T.Q. Hoang, V. Pikov, E. Meng, J. Neural Eng. **10**, 045002 (2013)
D.R. Kipke, W. Shain, G. Buzsáki, E. Fetz, J.M. Henderson, J.F. Hetke, G. Schalk, J. Neurosci. **28**, 11830 (2008)
N. Kishi, W.F. Chen, Y. Goto, J. Struct. Eng. **123**, 313 (1997)
T.D.Y. Kozai, N.B. Langhals, P.R. Patel, X. Deng, H. Zhang, K.L. Smith, J. Lahann, N.A. Kotov, D.R. Kipke, Nat. Mater. **11**, 1065 (2012a)
T.D.Y. Kozai, A.L. Vazquez, C.L. Weaver, S.-G. Kim, X.T. Cui, J. Neural Eng. **9**, 066001 (2012b)
A. Leskovar, L. Moriarty, J. Turek, I. Schoenlein, R. Borgens, J. Exp. Biol. **203**, 1783 (2000)
D. Lewitus, K.L. Smith, W. Shain, J. Kohn, Acta Biomater. **7**, 9 (2011)
Y. Lu, T. Li, X. Zhao, M. Li, Y. Cao, H. Yang, Y.Y. Duan, Biomaterials **31**, 5169 (2010)
T. Lund, S.E. Hermansen, T.V. Andreasen, J.O. Olsen, B. Østerud, T. Myrmel, K. Ytrehus, Thromb. Haemost. **104**, 582 (2010)
A. Mercanzini, P. Colin, J.C. Bensadoun, A. Bertsch, P. Renaud, IEEE Trans. Biomed. Eng. **56**, 1909 (2009)
C. Ming, G. Xiaorong, G. Shangkai, X. Dingfeng, Biomed. Eng. IEEE Trans. **49**, 1181 (2002)
J.K. Nguyen, D.J. Park, J.L. Skousen, A.E. Hess-Dunning, D.J. Tyler, S.J. Rowan, C. Weder, J.R. Capadona, J. Neural Eng. **11**, 056014 (2014)
J.N. Patel, B. Kaminska, B.L. Gray, B.D. Gates, J. Micromech. Microeng. **18**, 095028 (2008)

G. Pfurtscheller, C. Neuper, C. Guger, W. Harkam, H. Ramoser, A. Schlogl, B. Obermaier, M. Pregenzer, Rehabil. Eng. IEEE Trans. **8**, 216 (2000)
V.S. Polikov, P.A. Tresco, W.M. Reichert, J. Neurosci. Methods **148**, 1 (2005)
R. Rojas, N.K. Harris, K. Piotrowska, J. Kohn, J. Polym. Sci. A Polym. Chem. **47**, 49 (2009)
P.J. Rousche, R.A. Normann, J. Neurosci. Methods **82**, 1 (1998)
M. Salcman, M.J. Bak, Biomed. Eng. IEEE Trans. **BME-20**, 253 (1973)
T. Saxena, L. Karumbaiah, E.A. Gaupp, R. Patkar, K. Patil, M. Betancur, G.B. Stanley, R.V. Bellamkonda, Biomaterials **34**, 4703 (2013)
E.M. Schmidt, M.J. Bak, J.S. McIntosh, Exp. Neurol. **52**, 496 (1976)
J. Schut, D. Bolikal, I. Khan, A. Pesnell, A. Rege, R. Rojas, L. Sheihet, N. Murthy, J. Kohn, Polymer (Guildf). **48**, 6115 (2007)
J.P. Seymour, D.R. Kipke, Biomaterials **28**, 3594 (2007)
C. Smith, K.D. Song, H. Yoon, W.-K. Kim, T. Zeng, L.D. Sanford, 834404 (2012)
T. Stieglitz, H. Beutel, C. Blau, J.U. Meyer, Biomed. Tech. **42**(Suppl), 449 (1997)
T. Sun, W.M. Tsang, W.-T. Park, K. Cheng, S. Merugu, Microsyst. Technol. (2014)
D.H. Szarowski, M.D. Andersen, S. Retterer, A.J. Spence, M. Isaacson, H.G. Craighead, J.N. Turner, W. Shain, Brain Res. **983**, 23 (2003)
S. Takeuchi, I. Shimoyama, J. Microelectromech. Syst. **9**, 24 (2000)
S. Takeuchi, T. Suzuki, K. Mabuchi, H. Fujita, in *Micro Electro Mech. Syst. 2003. MEMS-03 Kyoto. IEEE Sixt. Annu. Int. Conf.* (2003), pp. 367–370
S. Takeuchi, D. Ziegler, Y. Yoshida, K. Mabuchi, T. Suzuki, Lab Chip **5**, 519 (2005)
J.N. Turner, W. Shain, D.H. Szarowski, M. Andersen, S. Martins, M. Isaacson, H. Craighead, Exp. Neurol. **156**, 33 (1999)
T.M. Vaughan, W.J. Heetderks, L.J. Trejo, W.Z. Rymer, M. Weinrich, M.M. Moore, A. Kübler, B.H. Dobkin, N. Birbaumer, E. Donchin, E.W. Wolpaw, J.R. Wolpaw, IEEE Trans. Neural Syst. Rehabil. Eng. **11**, 94 (2003)
R.J. Vetter, J.C. Williams, J.F. Hetke, E.A. Nunamaker, D.R. Kipke, IEEE Trans. Biomed. Eng. **51**, 896 (2004)
J.H.-C. Wang, B.P. Thampatty, Int. Rev. Cell Mol. Biol. **271**, 301 (2008)
T. Ware, D. Simon, D.E. Arreaga-Salas, J. Reeder, R. Rennaker, E.W. Keefer, W. Voit, Adv. Funct. Mater. **22**, 3470 (2012)
J.C. Williams, R.L. Rennaker, D.R. Kipke, Brain Res. Protocol. **4**, 303 (1999)
J.C. Williams, J.A. Hippensteel, J. Dilgen, W. Shain, D.R. Kipke, J. Neural Eng. **4**, 410 (2007)
K.D. Wise, J.B. Angell, A. Starr, Biomed. Eng. IEEE Trans. **BME-17**, 238 (1970)
T. Zhu, P. Argyrakis, E. Mastropaolo, K.K. Lee, R. Cheung, J. Vac, Sci. Technol. B Microelectron. Nanom. Struct. **25**, 2553 (2007)